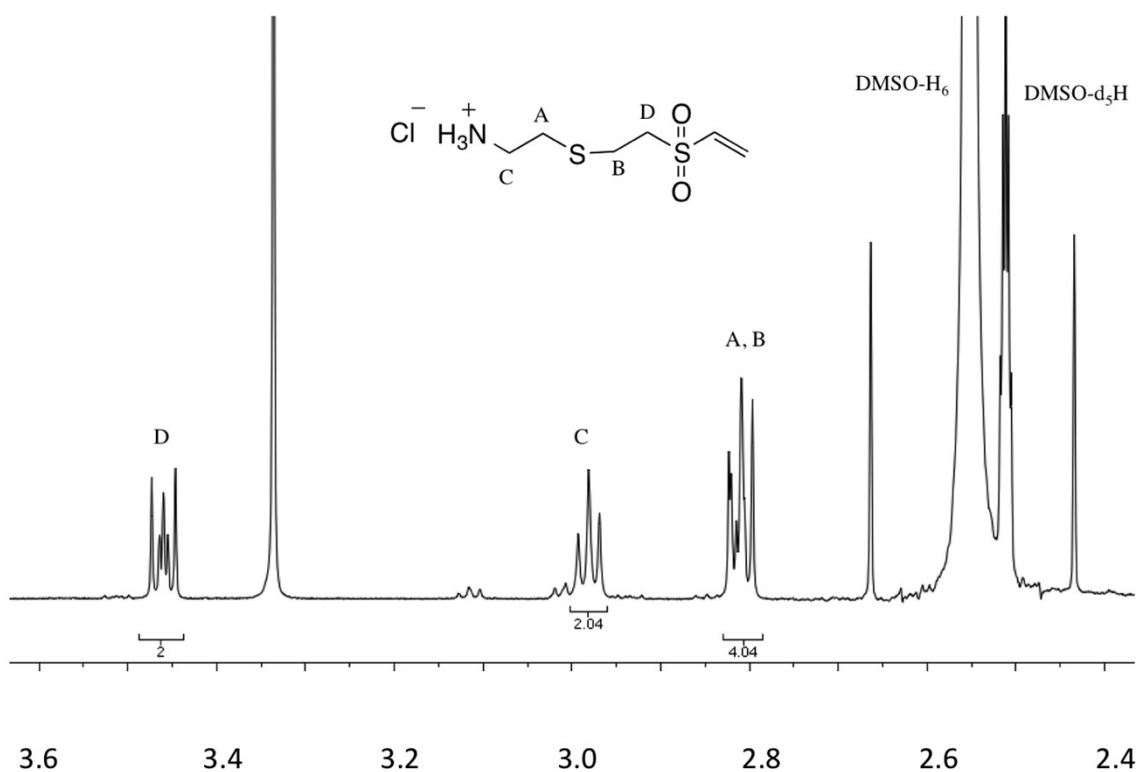


Supplementary Information

Synthetic Hydrogels formed by Thiol-Ene Crosslinking of Vinyl Sulfone-functional  
Poly(Methyl Vinyl Ether-*alt*-Maleic Acid) with  $\alpha,\omega$ -Dithio-Polyethyleneglycol

S. Alison Stewart, Michael B. Coulson, Christal Zhou, Nicholas A.D. Burke, Harald D. H.  
Stöver\*

Department of Chemistry and Chemical Biology  
McMaster University, Hamilton, Ontario, Canada



**Figure S-1:** <sup>1</sup>H NMR spectrum of crude CVS-HCl in DMSO/DMSO-d<sub>6</sub>, focused on the aliphatic region ( $\delta$ 3.6 to  $\delta$ 2.4).

To assess the progress of the cysteamine divinyl sulfone Michael addition (Figure S-1), a drop of the crude mixture in DMSO was diluted in DMSO-d<sub>6</sub> giving rise to the dual peaks at  $\delta$ 2.5 from both DMSO-H<sub>6</sub> and DMSO-d<sub>5</sub>H. Near-quantitative conversion of cysteamine to cysteamine vinyl sulfone HCl was determined by the ethylene integrations

4:2:2 (A+B:D:C), and the near disappearance of cysteamine ethylene signals at  $\delta$ 3.1 and  $\delta$ 3.0.

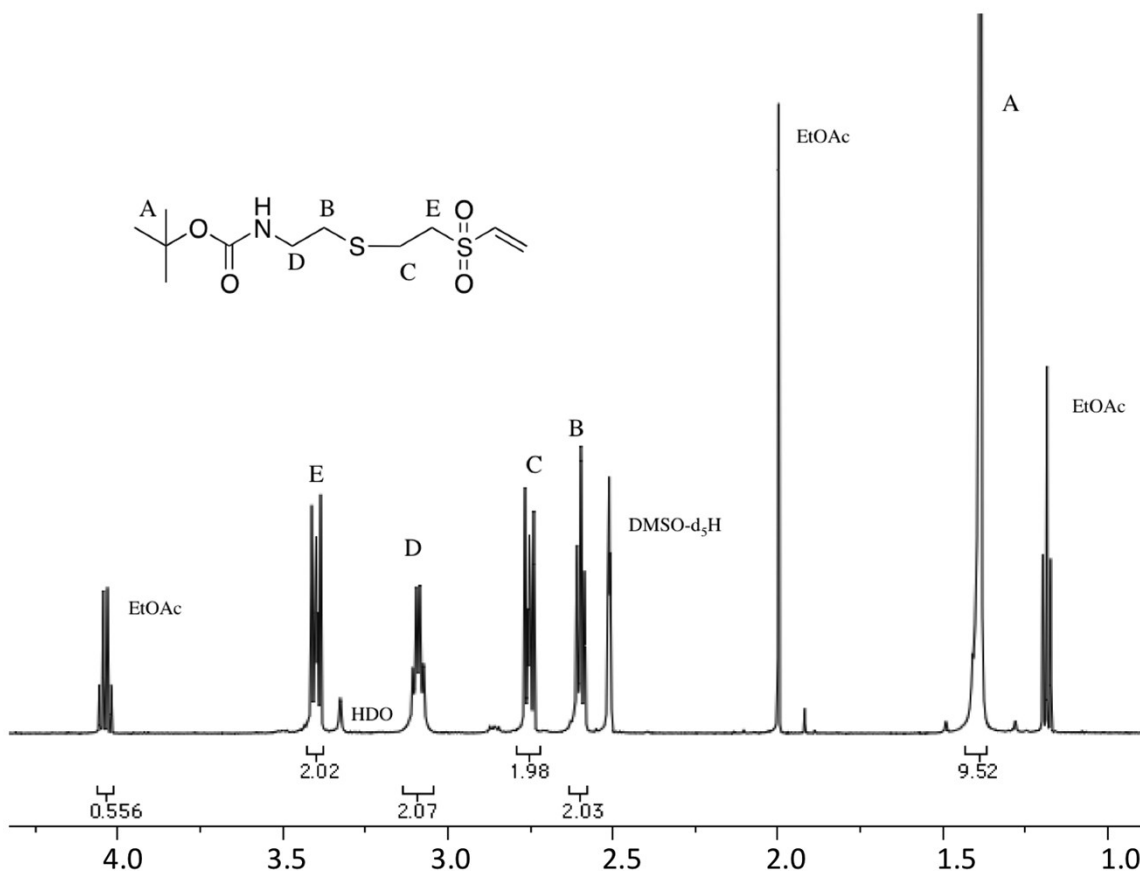


**Figure S-2:** <sup>1</sup>H NMR spectrum of isolated N-BOC CVS in DMSO-d<sub>6</sub>, focused on the aliphatic region ( $\delta$ 4.25 to  $\delta$ 1.0).

<sup>1</sup>H NMR confirmed the presence of the tert-butyl signal of the BOC protecting group ( $\delta$ 1.4, 9H, s) with an area consistent with complete amine protection, as well as the downfield shift of the methylene adjacent to the N-atom. Note the divergence of the peaks from protons adjacent to the thioether following protection.

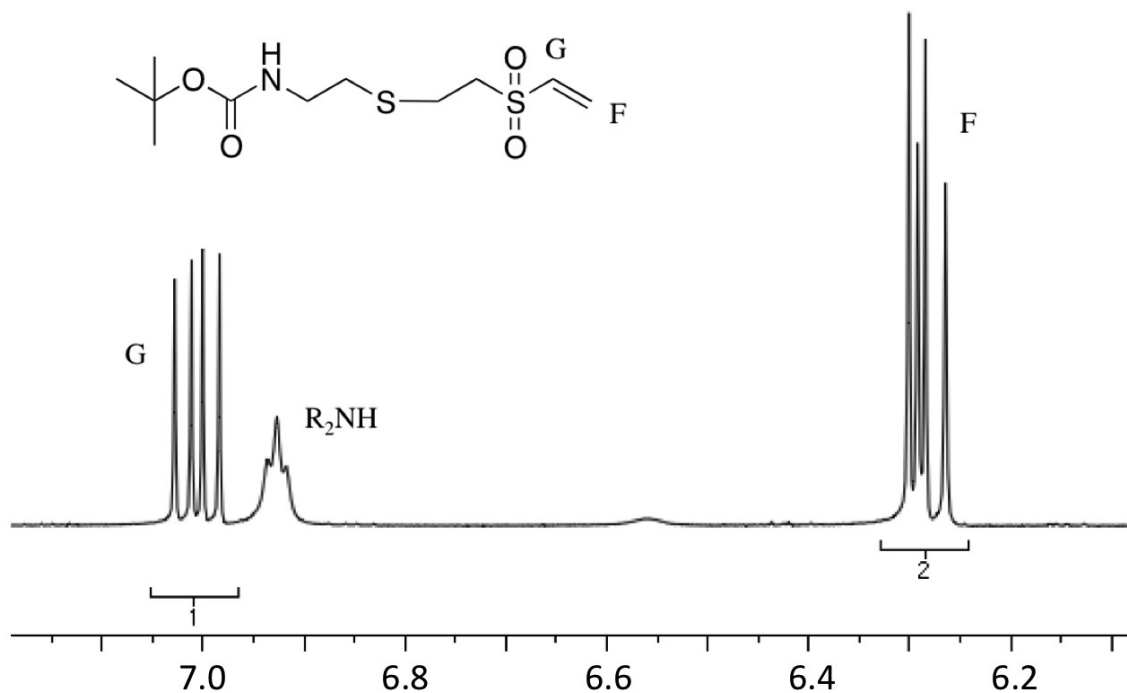


**Figure S-3:** <sup>1</sup>H NMR spectrum of N-BOC CVS in DMSO-d<sub>6</sub>, focused on the vinyl region (δ7.2 to δ6.1).

Ethyl acetate, used as column eluent, was present in the N-BOC CVS sample (Figure S-2), however it was removed in subsequent steps. The presence of the triplet at δ6.9 also affirms presence of the N-BOC linkage, as the aprotic solvent allows for the retention of the NH proton (Figure S-3). No peaks were seen between δ6.1 - 4.25.

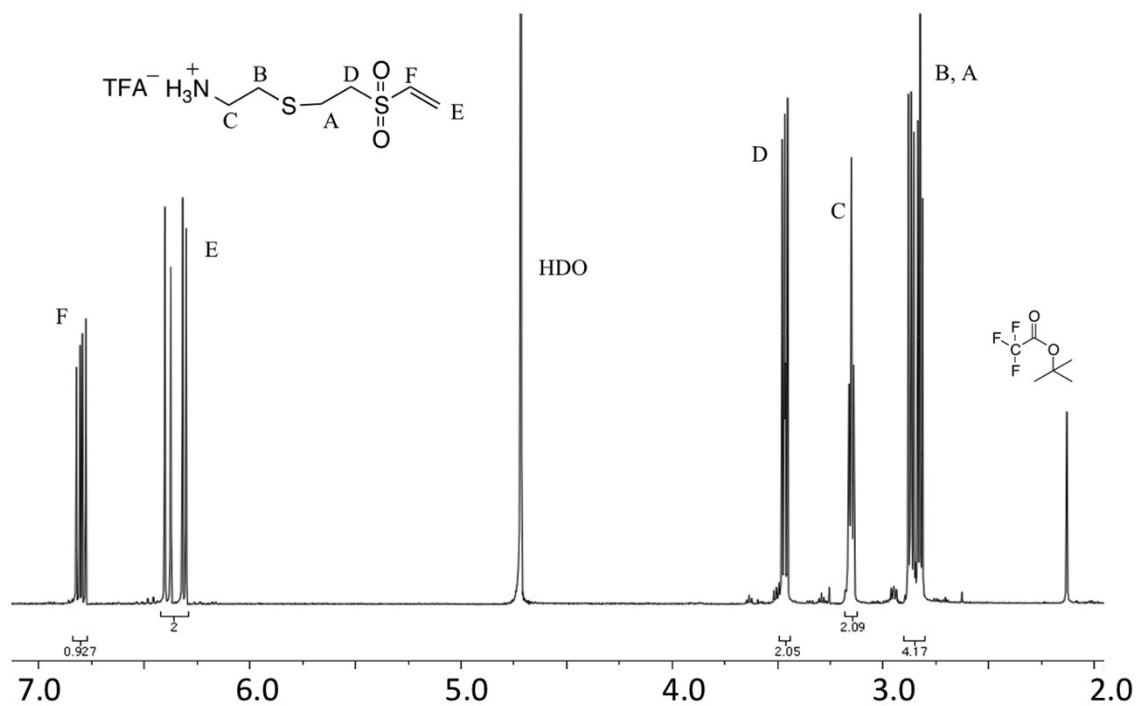


**Figure S-4:** <sup>1</sup>H NMR spectrum of CVS TFA in D<sub>2</sub>O.

Deprotection of N-BOC CVS to form the final CVS TFA product was confirmed by the disappearance of the *t*-butyl signal ( $\delta$ 1.4, 9H, s), as well as the convergence of the proton environments A and B (Figure S-4), leading to a similar spectrum as CVS·HCl. *t*-Butyl trifluoroacetate, a side product from the preceding TFA deprotection, was present in this sample ( $\delta$ 2.2).

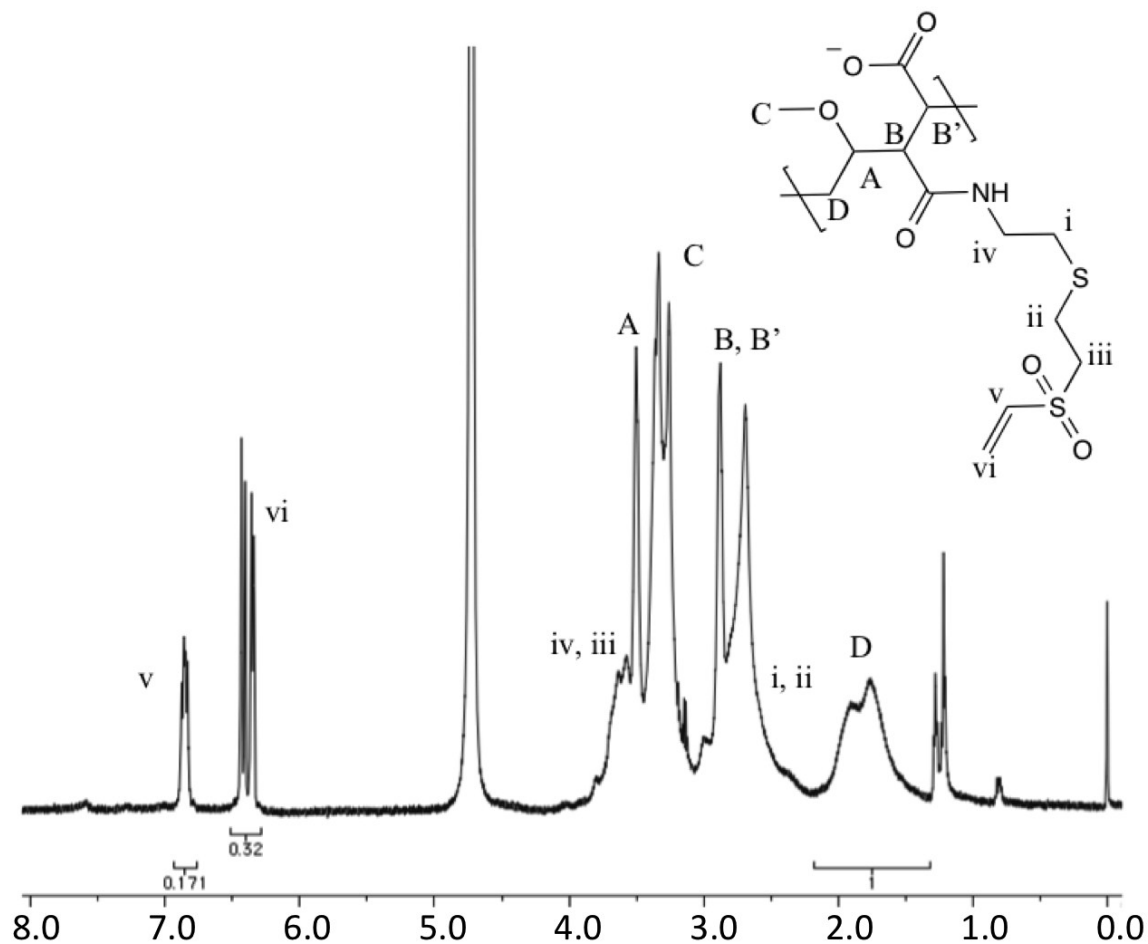


**Figure S-5:**  $^1\text{H}$  NMR spectrum of PMM-CVS<sub>30</sub> in  $\text{D}_2\text{O}$ . The ratio of grafted CVS groups was determined by vinyl signal integration (v, 1H,  $\delta$ 6.8; vi, 2H,  $\delta$ 6.4) compared to the backbone methylene peak (D, 2H,  $\delta$ 1.5-2).

PMM-CVS <sub>10</sub>		PMM-CVS <sub>20</sub>		PMM-CVS <sub>30</sub>	
Target	Actual	Target	Actual	Target	Actual
15	11	25	19	35	32

**Table S-1:** Degree of substitution of PMM-CVS<sub>x</sub> polymers comparing target to outcome percentage, and the shorthand used to denote polymer functionalization.

There is some uncertainty in integration due to the broad signal of the polymeric methylene internal standard, as well as variations in vinylic peaks, from impurities present in the purchased PMMA. Due to these integration variations, ratios were rounded to the nearest ten, and denoted as such (Table S-1). Sodium chloride (0.05 M) was added to the first two dialysis baths, successfully displacing ionically bound cations, TEA and CVS.



**Figure S-6:** Image of as formed PMM-CVS<sub>30</sub>-f 5% w/v HS-PEG-SH hydrogel, demonstrating high transparency.

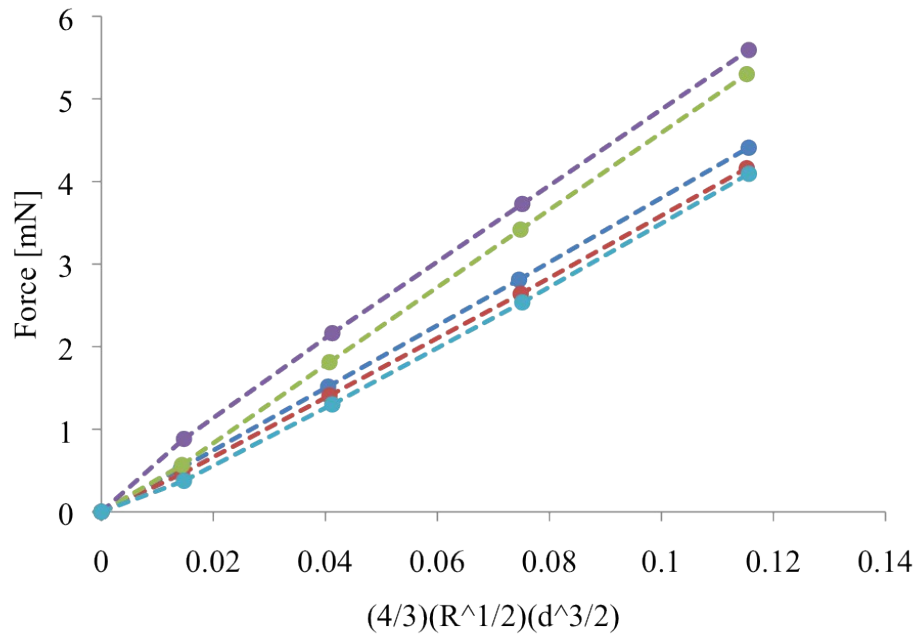


**Figure S-7:** Force strain curve for PMM-CVS<sub>20</sub> 7.5% w/v HS-PEG-SH hydrogel.

In order to calculate the Young's modulus from contact stress, the measured force from indentation was plotted against displacement ( $d^{3/2}$ ) multiplied by a constant ( $[(4/3)[R^{1/2}]])$  and fitted to by Hertzian theory. The slope of the strain curve ( $E^*$ ) was multiplied by Poisson's ratio ( $\nu$ ) [ $1/E^* = (1-\nu)/E$ ], assumed to be 0.5 for elastically deformed materials, where  $E$  is the Young's modulus ( $E$ ).

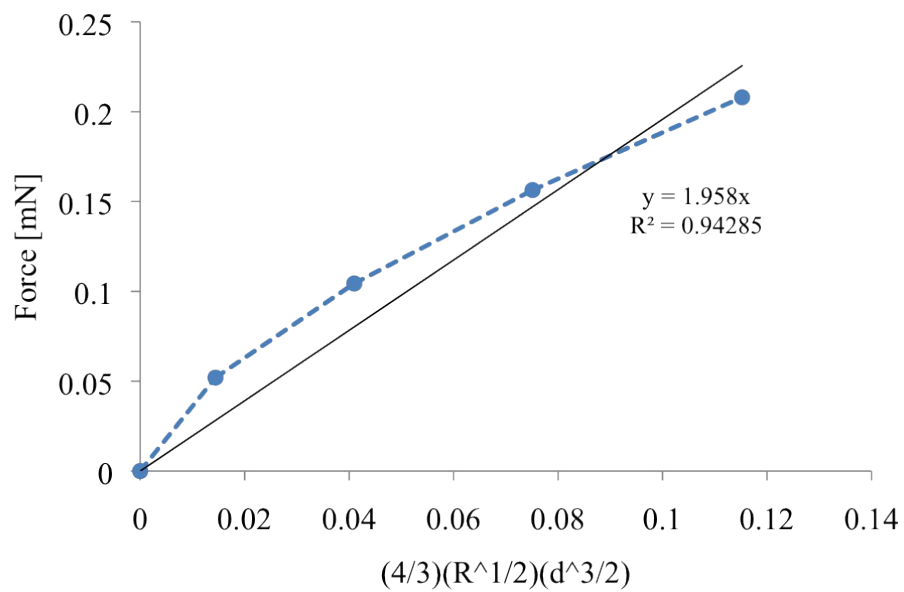


**Figure S-8:** Force strain curve for PMM-CVS<sub>10</sub> 7.5% w/v HS-PEG-SH hydrogel, swollen in PBS buffer for 7 days, demonstrating fast relaxation after contact stress.

Highly swollen gels exhibited creep compliance under contact stress, even at high deformation speeds, shown by the concave nature of the force-strain curve. Curves with  $R^2$  values lower than 0.98 were not used in calculation of Young's modulus average.

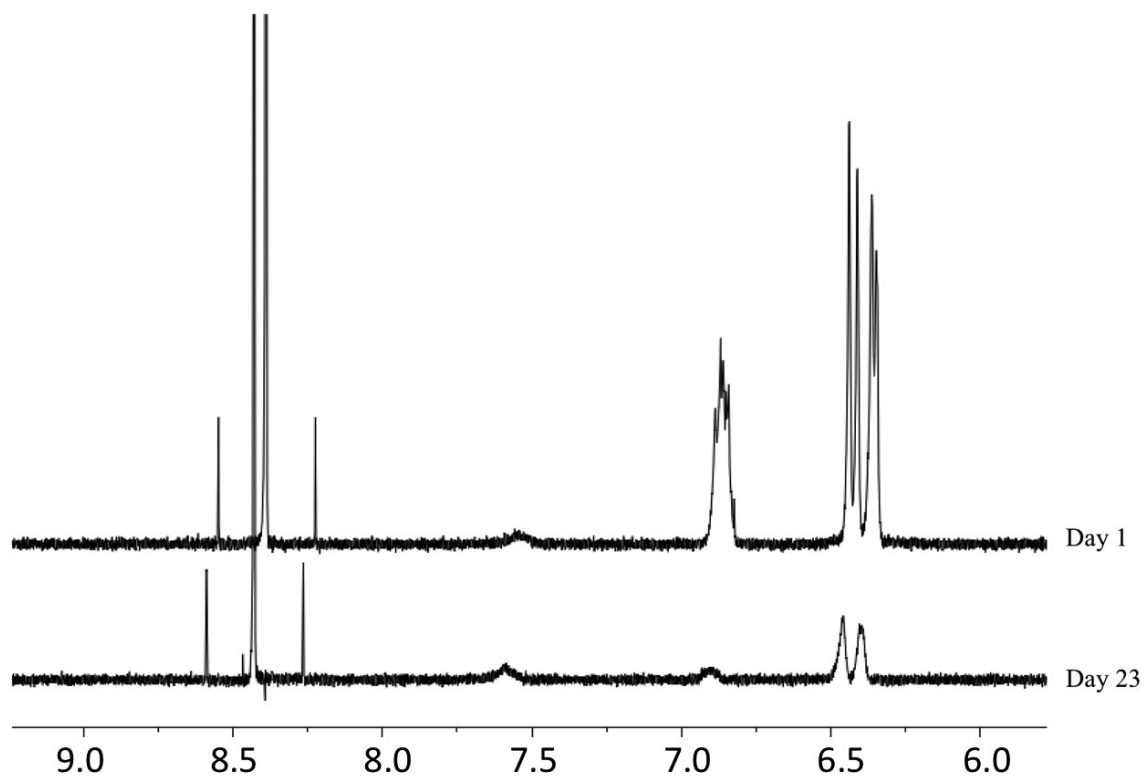


**Figure S-9:** Vinyl region (horizontally offset) of the <sup>1</sup>H NMR spectra of PMM-CVS<sub>30</sub> fixed at pD 7.7 and 37 °C. Spectra at Day 1 and Day 23 are shown. The signal at 8.4 ppm is due to formic acid added as a standard

The stability of polymer-bound vinyl groups was monitored by <sup>1</sup>H NMR, over a period of 23 days. Displayed in Figure S-9 are the first and final spectra of the profile, which show vinyl signals from the polymer ( $\delta$ 6.8 and  $\delta$ 6.4), formic acid internal standard ( $\delta$ 8.4) and vinylic impurity ( $\delta$ 7.6). The loss of the vinyl signal is thought to be due to hydration of the double bond.

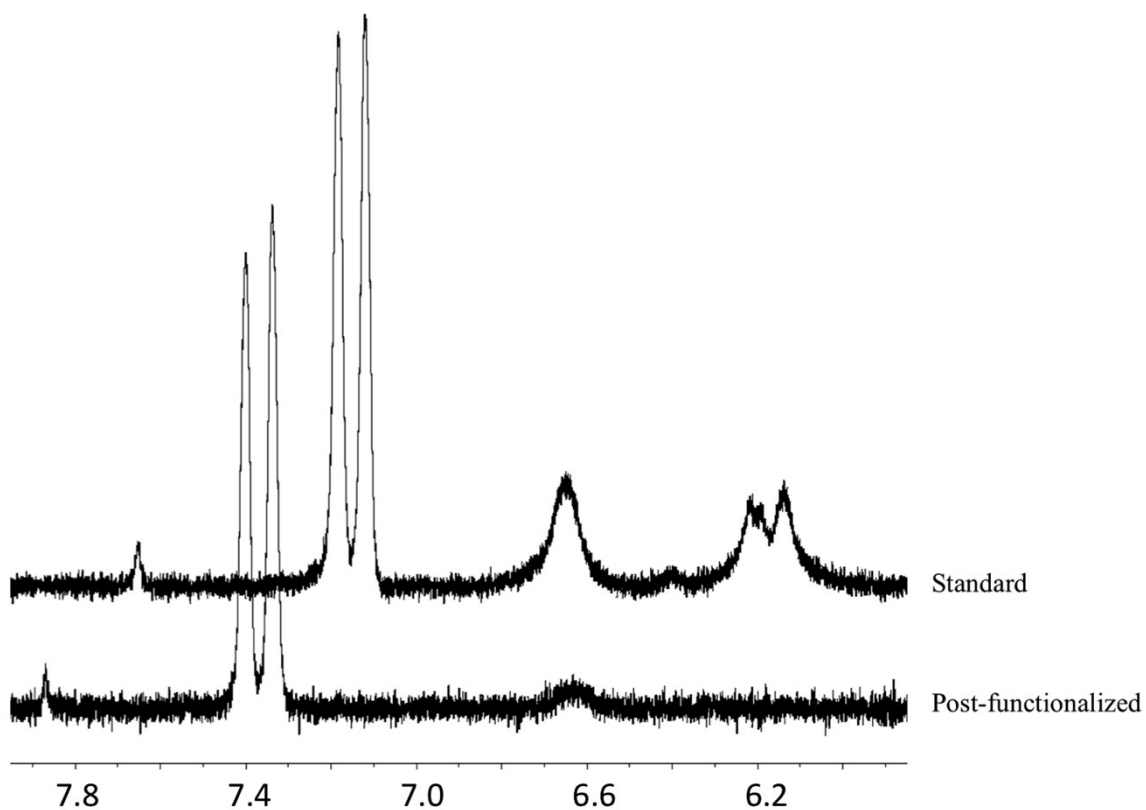


**Figure S-10:** Post-functionalization using cysteamine of 50% crosslinked PMM-CVS<sub>30</sub> 5% w/v HS-PEG-SH. Displayed is a vinyl region of the resulting <sup>1</sup>H NMR spectrum, before (standard), and after (post-functionalized) cysteamine addition. The sharp peaks near 7.4 ppm are due to phthalate added as an internal standard.

In order to determine the degree of post functionalization via the addition of small molecules, a standard was monitored and no change in integration was seen over the period of post-functionalization (Figure S-8). To integrate the vinyl region of the post functionalized spectrum, both peaks ( $\delta$ 6.8 and  $\delta$ 6.4) were analyzed separately, leaving out the vinylic impurity ( $\delta$ 6.65). The signals from the internal reference standard, PHT, can be seen at  $\delta$ 7.4.

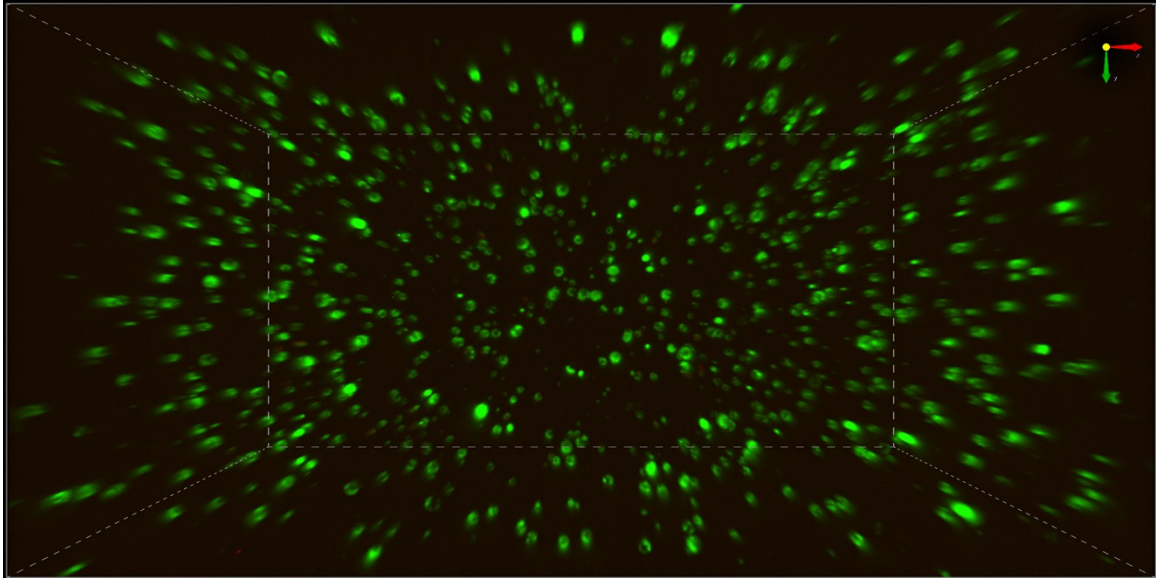


**Figure S-11:** 1000  $\mu\text{m}$  thick z-stack obtained using Nikon Eclipse Ti confocal microscope of the central portion of a 5% w/v PMM-CVS<sub>20</sub> HS-PEG-SH hydrogel, illustrating homogeneous distribution of cells throughout the gel.

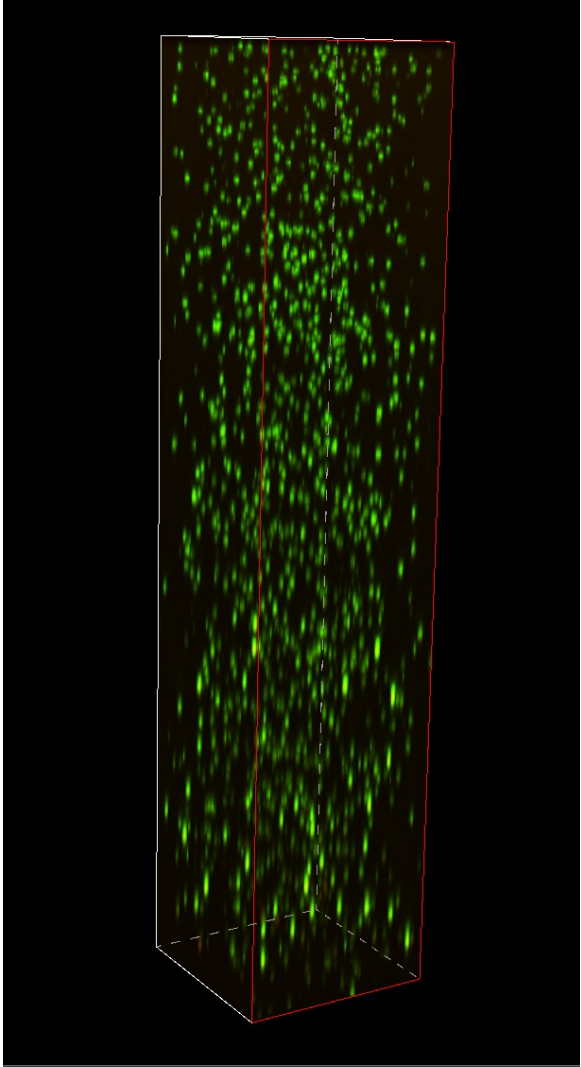


**Figure S-12:** 2500  $\mu\text{m}$  thick z-stack obtained using Nikon Eclipse Ti confocal microscope of the full depth of a 5% w/v PMM-CVS<sub>20</sub> HS-PEG-SH hydrogel, demonstrating homogeneous distribution of cells throughout the gel. The bottom of the image corresponds to the physical well-bottom.